Glassy dynamics of polymethylphenylsiloxane in one- and two-dimensional nanometric confinement—A comparison

Wycliffe K. Kipnusu, Mohamed Elsayed, Reinhard Krause–Rehberg, and Friedrich Kremer

Citation: The Journal of Chemical Physics **146**, 203302 (2017); doi: 10.1063/1.4974767
View online: https://doi.org/10.1063/1.4974767
View Table of Contents: http://aip.scitation.org/toc/jcp/146/20
Published by the American Institute of Physics

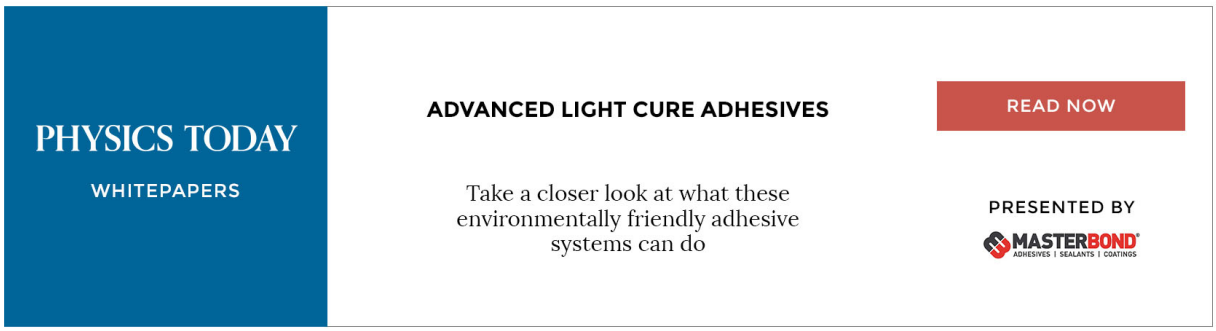

Glassy dynamics of polymethylphenylsiloxane in one- and two-dimensional nanometric confinement—A comparison

Wycliffe K. Kipnusu,[1,a)] Mohamed Elsayed,[2,3] Reinhard Krause–Rehberg,[2] and Friedrich Kremer[1]
[1]*Institute of Experimental Physics I, University of Leipzig, 04103 Leipzig, Germany*
[2]*Department of Physics, Martin Luther University Halle, 06099 Halle, Germany*
[3]*Department of Physics, Faculty of Science, Minia University, 61519 Minia, Egypt*

(Received 3 November 2016; accepted 14 December 2016; published online 2 February 2017)

Glassy dynamics of polymethylphenylsiloxane (PMPS) is studied by broadband dielectric spectroscopy in one-dimensional (1D) and two-dimensional (2D) nanometric confinement; the former is realized in thin polymer layers having thicknesses down to 5 nm, and the latter in unidirectional (thickness 50 μm) nanopores with diameters varying between 4 and 8 nm. Based on the dielectric measurements carried out in a broad spectral range at widely varying temperatures, glassy dynamics is analyzed in detail in 1D and in 2D confinements with the following results: (i) the segmental dynamics (dynamic glass transition) of PMPS in 1D confinement down to thicknesses of 5 nm is identical to the bulk in the mean relaxation rate and the width of the relaxation time distribution function; (ii) additionally a well separated surface induced relaxation is observed, being assigned to adsorption and desorption processes of polymer segments with the solid interface; (iii) in 2D confinement with native inner pore walls, the segmental dynamics shows a confinement effect, i.e., the smaller the pores are, the faster the segmental dynamics; on silanization, this dependence on the pore diameter vanishes, but the mean relaxation rate is still faster than in 1D confinement; (iv) in a 2D confinement, a pronounced surface induced relaxation process is found, the strength of which increases with the decreasing pore diameter; it can be fully removed by silanization of the inner pore walls; (v) the surface induced relaxation depends on its spectral position only negligibly on the pore diameter; (vi) comparing 1D and 2D confinements, the segmental dynamics in the latter is by about two orders of magnitude faster. All these findings can be comprehended by considering the density of the polymer; in 1D it is assumed to be the same as in the bulk, hence the dynamic glass transition is not altered; in 2D it is reduced due to a frustration of packaging resulting in a higher free volume, as proven by *ortho*-positronium annihilation lifetime spectroscopy. *Published by AIP Publishing.* [http://dx.doi.org/10.1063/1.4974767]

I. INTRODUCTION

The investigation of the dynamic glass transition of polymers confined in thin films, i.e., one-dimensional (1D) confinement where the molecular mobility is constraint only in the direction normal to the film plane, witnessed an era of extremely active research in the past two decades. For this type of confinement, numerous experimental and theoretical studies of polymers in thin layers were carried out[1–3] with the central conclusion that with linear response methods, like broadband dielectric spectroscopy (BDS) or AC-calorimetry, no confinement effects could be detected, while for measurements in the non-equilibrium state widely varying results are obtained.[2,3] Much less is known concerning the dynamics of polymers in two-dimensional (2D) constraints being contained in nanoporous systems like sol-gel glasses,[4] zeolites,[5] or soft matrices.[6] The main disadvantage of these host systems is the fact that the topology of the inner surfaces is not well characterised. In the meantime, this limitation is eliminated by the possibility to produce silica membranes having unidirectional channels with diameters as small as 4 nm and with a thickness of 50 μm. By that it is possible to compare quantitatively the dimensionality of the confinement on the glassy dynamics.

In this article, we compare the dynamics of polymethylphenylsiloxane (PMPS) under 1D and 2D geometrical constraints. The results show that the dynamic glass transition of PMPS is not affected by the 1D confinement but it is strongly influenced if it is restricted in the 2D geometries in the form of nanopores where the glassy dynamics becomes faster as the average pore diameters decrease. This is attributed to the reduction in the packing density which is corroborated by the positron annihilation lifetime spectroscopy (PALS). The overall findings underpin the importance of the dimensionality in the understanding of macromolecules in constrained environments.

II. MATERIALS AND EXPERIMENTAL DETAILS

The PMPS (hydroxyl terminated) with a molecular weight of 2530 g/mol was obtained from polymer source. The thin films were prepared by spin coating the PMPS solution onto a silicon substrate. The substrates were initially covered with a

a)Electronic mail: kipnusu@physik.uni-leipzig.de

700 nm thick protective layer of photoresist (microresist technology GmbH). They were then cut along the crystallographic axes in small rectangular pieces of 4×10 mm^2. After cutting, the photoresist layer was removed in an ultrasonic bath of pure acetone and then dried with compressed nitrogen. As a second step, the cleaned substrates were inserted into a plasma cleaner (Plasma cleaner Femto timer) for about 5 min and then placed on top of a hot plate (at 150 °C) followed by cleaning with supercritical CO_2 (Applied Surface Technologies). The PMPS was dissolved in toluene and then spin coated (at 3000 rpm for 20 s) onto the clean silicon wafers. Different film thicknesses were obtained by varying the concentration of the PMPS in the solutions. The film thickness was measured with 1–2 nm precision by analyzing atomic force microscopy images of scratches applied to the polymer film with a stainless steel needle. To remove any residual solvent molecules and to eliminate stress imposed by the spin-coating procedure, all polymer films were annealed for 48 h at 423 K in oil free high vacuum (10^{-6} mbar) before performing the BDS measurements. The sample setup with novel nanostructured counter electrodes employed in the current work (Fig. 1(a), top panel) was used for the BDS measurements. This counter electrode contains a regular matrix of insulating silica nanostructures (acting as spacers) attached onto a highly conductive and polished silicon wafer. The quadratic nano-spacers (Fig. 1(a), bottom) have lateral dimensions of 5 μm and different heights ranging from 100 to 35 nm. By keeping the sample thicknesses much smaller than the spacer height, a free upper interface (air) is realized (Fig. 1(a), top panel). This arrangement circumvents the problem of electrical shorts and possible artefacts that can result from evaporated metal electrodes enabling the BDS measurement of ultra thin films[7] or even isolated polymer coils.[8] To check the reproducibility of the BDS measurements, the complex dielectric permittivity was monitored on heating and cooling cycles.

The nanoporous silica (pSi) membranes were prepared by the electrochemical etching of highly doped (0.005 Ω cm) p-type ⟨100⟩ oriented mono-crystalline silicon wafers in a home built anodization cell for use in the 2D confinements. The electrolyte contained hydrofluoric acid (HF-48%) and ethanol (C_2H_5OH-99%) purchased from Sigma-Aldrich and mixed in the ratio of 1:1. Current densities (j) in the range of 20–120 mA cm^{-2} were applied to obtain pore diameters between 4 and 10 nm with porosity varying from 9% to 23%. In each case, the etching time was adjusted to maintain the thickness of the pSi at around 50 μm. As the final electro-polishing step (j = 700 mA cm^{-2}) was applied for 3–4 s to lift the pSi from the Si substrate. The obtained pSi membranes were subsequently oxidized thermally in an oven (Vulcan 3-550, Neytech) at 1100 K (heating rate 3 K/min) for 6 h to form completely transparent and insulating nanoporous silica ($pSiO_2$) with unidirectional pores. The scanning electron micrograph (SEM) image of the cross section of pSi (Fig. 1(b), top left) reveals non-intersecting pores. The SEM image of the top surface of $pSiO_2$ is shown in Fig. 1(b) (top right). The pore size distribution as revealed by nuclear magnetic resonance (NMR) cryoporometry is depicted in Fig. 1(b) (bottom). Another set of the prepared $pSiO_2$ was silanized by reacting with the hexamethyldisilane (HMDS) (purity 99.9%, purchased from Sigma-Aldrich) in the vacuum chamber at 350 K for 6 h and later evacuated to remove the unreacted HMDS.

Before filling the membranes with the material under study, they were annealed in a high vacuum chamber (10^{-6} mbar) at 573 K for 24 h to remove water and other volatile impurities. The temperature was then decreased to 300 K before the probe sample (liquid) was injected into the closed vacuum where the pores were filled by capillary wetting. The natural rubber (which is used only once) ensures that the vacuum chamber remains air tight even after the injection of the sample. A similar procedure was used during silanization with the exception that the vacuum chamber was evacuated to get rid of the ungrafted HDMS (as described above) before injecting the probe sample. With this approach, we achieved complete filling of the nanopores with the investigated sample as confirmed by gravimetric and PALS measurements.

Dielectric measurements were carried out using a high-resolution Alpha analyser equipped with a Quatro temperature controller ensuring temperature stability better than 0.1 K within a temperature range of 350–200 K and a frequency window of 10^{-2}–10^7 Hz.

A fast-fast coincidence system with a time resolution of 215 ps[9] was used to perform PALS measurement. A sandwich

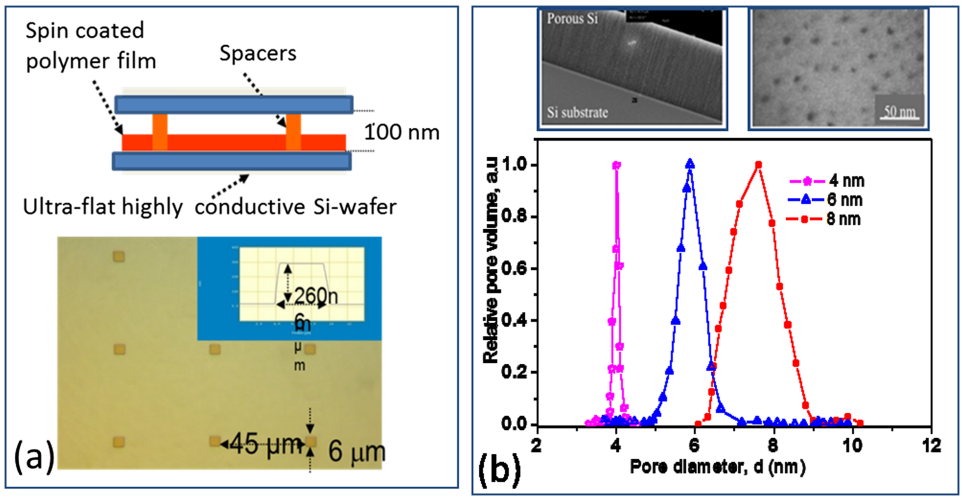

FIG. 1. (a) Scheme of a nanostructured electrode arrangement, in which one-dimensional nanometric confinement can be realized (top), optical image of the nano spacer arrays on the silicon wafer counter electrode with a cross section of the single nano spacer obtained from atomic force microscopy (b) Unidirectional silica nanopores to realize two dimensional confinement: Scanning Electron micrograph (SEM) of a cross section of an etched silicon showing non-intersecting nanopores (top left), SEM image of the surface nanoporous silica (top right), pore size distribution obtained by NMR cryoporometry for the nanoporous silica (bottom).

of the positron source (20 μ Ci ^{22}Na) between nanoporous silica layers (≈500 μm thick) with either empty pores or filled with PMPS was wrapped in a Kapton foil and placed in a hermetically sealed sample holder in a vacuum chamber (10^{-6} mbar) containing a cooling system. The samples were measured in the temperature range 180–340 K in steps of 5 K. 4–5 × 10^6 counts were accumulated in each positron lifetime spectrum. Source contribution of 13.8% was determined by measuring a silicon reference sample (218 ps). After source and background corrections, the positron lifetime spectra were analyzed by the lifetime LT 9 program[10] to three components which arise from the annihilation of *para*–positronium (Ps) (τ_1 = 125–150 ps), free positrons (τ_2 = 350–450 ps), and *ortho*–Ps pickoff (τ_3 = 1.5–3.5 ns).

III. RESULTS AND DISCUSSIONS

The representative isothermal dielectric loss spectra of the PMPS in the bulk state for a few selected temperatures are shown in Fig. 2(a). These data were fitted to the empirical Havriliak-Negami function[5] given by

$$\varepsilon^*_{HN}(\omega) = \varepsilon_\infty + \frac{\Delta\varepsilon}{[1 + (i\omega\tau_{HN})^\alpha]^\gamma} + \frac{\sigma_0}{i\omega\varepsilon_0}, \quad (1)$$

where $\Delta\varepsilon$ is the dielectric relaxation strength, τ_{HN} is the characteristic time constant, which is related to the relaxation time at maximum loss[5] (τ_{max}), σ_0 is the dc-conductivity, ε_0 is the permittivity of free space, and $0 < \gamma, \gamma\alpha \leq 1$ represent the broadening of the loss peaks. A comparison of the isochronal dielectric spectra of PMPS in the bulk state and under 1D geometrical constraints of thin films down to 5 nm depicted in Fig. 2(b) shows that the segmental dynamics of PMPS in thin films is neither shifted nor broadened with respect to the bulk sample. However, another well separated process which is much broader than the segmental mode appears at higher temperatures for the confined sample. We ascribed this process to the surface interactions (adsorption and desorption) of the polymer chains at the polymer/substrate interface involving the silanol groups of the native thin silica layer on the silicon wafers. The intensity of this process, as observed in Fig. 2(b), increases with decreasing film thickness due to the fact that the ratio of the number density of the dipolar units involved in this process compared to the segmental mode increases as the film thickness decreases. We restrained from analysing the dielectric strength (related to the observed intensities) of these processes due to the fact that the sample geometry employed for the measurement of the thin films introduces significant uncertainties in the determination of this quantity. We therefore do not quantitatively discuss the dielectric strength in this manuscript.

In terms of the relaxation times, the surface induced mode for the thicker films (31 nm) (Fig. 3) is slower compared to that of 14 and 5 nm thick films whose relaxation rates are nearly identical in a wide temperature range. However, they all tend to merge as the calorimetric glass transition temperature is approached while following a Vogel–Fulcher–Tammann (VFT) type of thermal activation represented by

$$\tau_{max} = \tau_\infty \exp\left(\frac{DT_0}{T - T_0}\right), \quad (2)$$

where τ_∞ is the high temperature limit of the relaxation time, D is the fragility parameter, and T_0 is the "ideal" glass transition temperature or the Vogel temperature. Interestingly, the relaxation rates of the segmental mode (related to the dynamic glass transition) are neither affected by the surface effects nor by the finite sizes of confinement as the data for the bulk and PMPS constrained in thin films of thicknesses down to 5 nm collapse into a single VFT (Eq. (2)) type dependence (Fig. 3).

This is rationalised by the fact that this mode involves fluctuations of very short section of the polymer chains corresponding to a lengthscale of about 0.5-1 nm and therefore would not be affected by the process taking place at the polymer/substrate interface at least for the film thicknesses studied in the current work. A sketch of the chains closer to this interface is shown in Fig. 4. Similarly, under 2D confinements in unidirectional silica nanopores, the surface induced mode whose intensity also increases with decreasing pore sizes is observed at higher temperatures for the native pores. This process is removed after silanization of the pores proving that it indeed originates from the interaction of the polymer chains with the confining surfaces (Fig. 5). Due to the surface curvature effects and the higher surface area to volume ratio, the segmental mode for PMPS in nanopores is broader compared to the bulk sample. The spectral peak position of this mode in nanopores is also shifted to lower temperatures implying faster dynamics due to confinement effects.

In order to analyse these effects in detail and to compare with the observations under 1D confinement, we fitted the isothermal dielectric loss spectra for all samples to the HN function (Eq. (1)). The obtained τ_{max} is plotted as shown in Fig. 6. From this analysis, we observe that (i) the surface induced mode is independent of the pore sizes and depicts an Arrhenius like type of thermal activation within the investigate temperature range, (ii) whereas the segmental mode for the bulk and in 1D confinement lies on a single VFT curve, that of 2D constrained PMPS deviates from the bulk and becomes

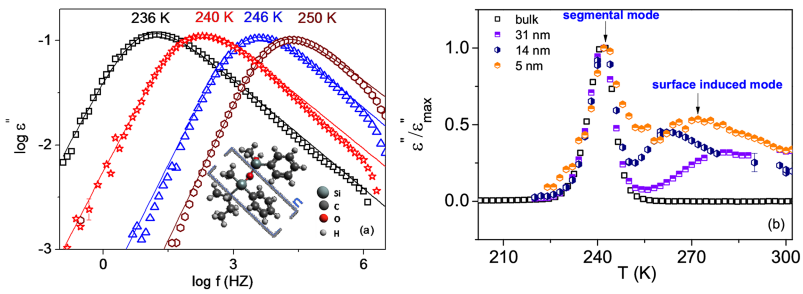

FIG. 2. Dielectric loss spectra for the bulk polymethylphenylsiloxane (PMPS) plotted as a function of frequency for the selected temperatures (a) and the isochronal spectra at a frequency of 120 Hz for PMPS confined in thin films (b). The lines in (a) are the Havriliak-Negami function (Eq. (1)) and the inset therein is the chemical structure of PMPS. The spectra in (b) are normalized with respect to the respective maximum peak of the segmental mode.

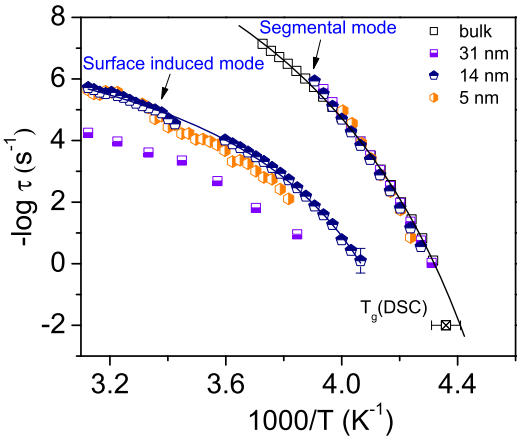

FIG. 3. Activation plots for the segmental and surface induced modes of PMPS confined in one-dimensional (1D) geometrical constraints in the form of nanometric thin films of thickness as indicated in the legend The relaxation times were obtained by fitting the isothermal dielectric loss data to the Havriliak-Negami function (Eq. (1)). The lines represent the VFT (Eq. (2)) fit to the data. The VFT fit parameters for the surface induced process with a film thickness of 14 nm are $\tau_\infty = 2.6 \times 10^{-4}$ s, $D = 1.3$, $T_0 = 212.3$ K, while those for bulk sample are $\tau_\infty = 3.2 \times 10^{-7}$ s, $D = 3.1$, $T_0 = 191.6$ K.

faster with decreasing pore sizes as T_g is approached. This deviation is more pronounced for the native pores, for instance, in 4 nm, it becomes nearly Arrhenius-like in its T-dependence. This was also observed in Refs. 4, 11, and 12, (iii) in silanized pores, the segmental dynamics reverts to the VFT dependence and is slower compared to the pristine silica pores but is still faster than the bulk by about two orders of magnitude. Similar observations have been found by several other experiments utilizing different techniques, such as Rayleigh light scattering,[13,14] neutron scattering,[15,16] optical Kerr effect spectroscopy,[17,18] nuclear magnetic resonance spectroscopy, and broadband dielectric spectroscopy,[4,11,19–23] to probe the dynamics of various low molecular weight glass formers confined in diverse porous media. The general finding is that the molecular dynamics under the 2D confinement realized in nanopores is governed by the interplay between the surface and confinement effects. We attribute the observations discussed above to the changes in the packing density of the constrained molecules which is reduced in 2D compared to the 1D confinement. To corroborate this supposition, we did positron annihilation lifetime spectroscopy (PALS) measurements of the bulk PMPS and when confined in native silica nanopores having average pore diameters of 4, 6, and 8 nm. The PALS technique is the most suited to quantify the intrinsic free volume (V_f) in a sample which is linked to the annihilation lifetime (τ_3) of the *ortho*-positronium via the Tao–Eldrup model.[24] In order to obtain τ_3 for PMPS confined in silica nanopores, we first measured the empty nanoporous silica layers to

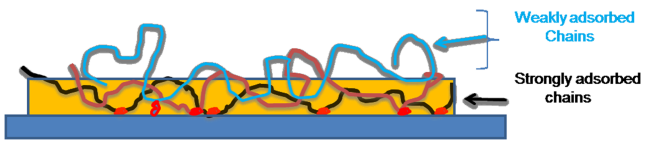

FIG. 4. Sketch of the PMPS chains spin coated on the silicon wafer illustrating the weakly and strongly adsorbed chains. The adsorption and desorption dynamics give rise to the surface induced process.

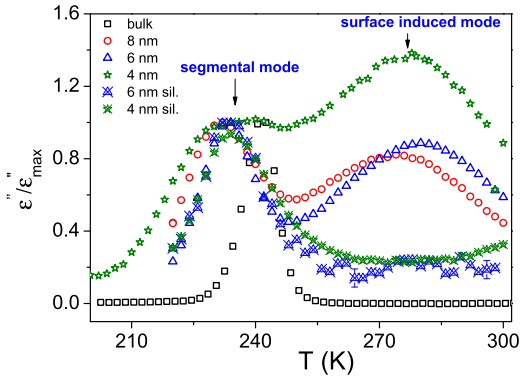

FIG. 5. Isothermal dielectric loss of PMPS confined in native and silanized silica nanopores. Each spectrum is normalized with respect to the maximum peak of its segmental mode. The surface induced mode is removed for the case of silanized pores.

determine the *ortho*-positronium lifetime (τ_3) and its relative intensity in the silica matrix. The positron lifetime spectra of these empty layers show 4 components; the first and second components are related to the *para*-Ps and free positrons, as mentioned above. The third component corresponds to the annihilation of *ortho*-Ps in silica matrix and the fourth is associated to the empty pores. We obtained a lifetime of τ_3 = 1.45–1.7 ns for the annihilation of the *ortho*-Ps in the silica matrix over the temperature range 180–340 K. This lifetime and its relative intensity are subtracted at each corresponding measurement temperature in the analysis of the porous samples filled with PMPS.

The T-dependence of the V_f for the investigated samples is depicted in Fig. 7 which shows higher values of V_f for PMPS confined in silica nanopores compared to the bulk sample. The change of slope of V_f at higher temperatures is due to the fact that τ_3 coincides with the structural relaxation time of the investigated polymer. This implies that the voids in the samples in which the positronium is trapped keep changing at a time scale that is equal or faster than the lifetime of the

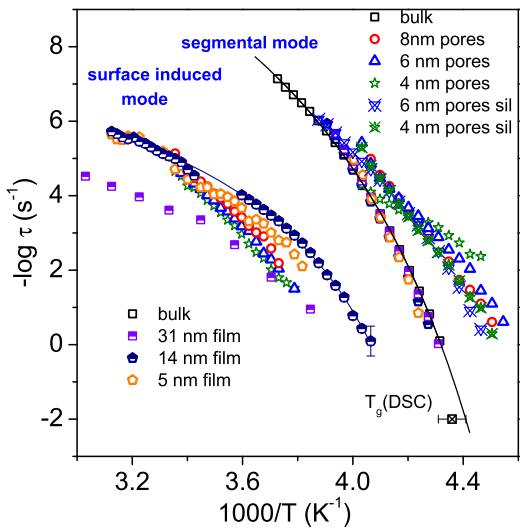

FIG. 6. Activation plots: A comparison of the relaxation rates of PMPS confined in thin films (1D) (half-filed symbols) and in native (open symbols) and silanized (crossed symbols) nanopores (2D) geometrical constraints.

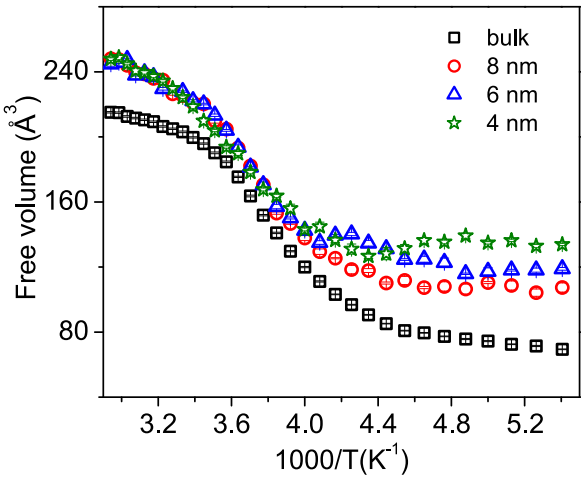

FIG. 7. The temperature dependencies of the free volume (V_f) obtained from *ortho*-positronium annihilation lifetime (τ_3) via the Tao–Eldrup model for the PMPS in the bulk state and when confined in nanopores with mean pore diameters of 4, 6, and 8 nm. The error bars are smaller than the symbols.

positronium decay. Consequently, the probe of the free volume within this temperature regime is rendered invalid. At the vicinity of the calorimetric glass transition of the bulk sample ($T_{g(bulk)} = 230$ K), the deviation of V_f for bulk and confined samples is higher and increases with decreasing pore diameters implying that the extreme confinement in 2D causes further frustration and reduction in the packing density. This corresponds to the temperature regime where the confinement effects of PMPS in nanopores are observed (Fig. 6). A combined PALS and BDS measurement of H-bonding system confined in native silica pores also showed similar results.[25] The vitrification of the interfacial layer would also reduce the effective pore volume of the bulk-like molecules at the centre of the pores, hence causing further frustration of the molecular packing leading to higher free volume and hence faster relaxation of the core molecules. This is supported by the observation that the segmental dynamics slows down after silanization of the silica nanopores. A comparison of the dynamics of 2D confined systems with strong surface interactions and the pressure dependence of the corresponding bulk samples led to the analogous conclusion that around $T_{g(bulk)}$, the 2D confined system enters into an isochoric state characterised by negative pressure which is implicitly related to the reduced packing density.[26,27]

An illustration of the polymer/substrate interactions (Fig. 8) shows that under 2D confinement, the polymer chains establish many more contact points with the substrate than the 1D constrained chains which would lead to different packing densities.

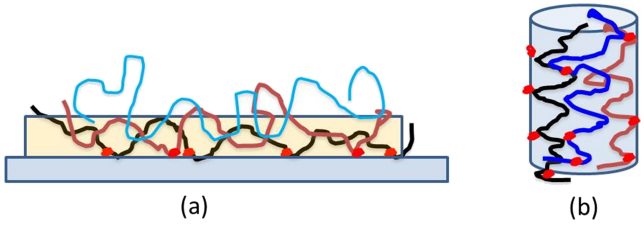

FIG. 8. Sketch of the PMPS chains constrained in thin films (a) and in nanopores (b).

IV. CONCLUSIONS

This article investigated the dynamics of PMPS under 1D and 2D geometrical constraints. The former case is realized when the polymer chains are confined in nanometric thin films while in the latter, the polymer is infiltrated into unidirectional silica nanopores. The BDS revealed two relaxation processes in each case: the surface induced mode which is related to the polymer/substrate interactions and the segmental mode that is connected to the dynamic glass transition. The surface induced mode does not affect the segmental mode which remains bulk-like both in its relaxation times and their distribution functions for the 1D confined PMPS. Conversely, the counter balance between the surface and confinement effects governs the dynamics under the 2D confinement. In this case, the confinement effects lead to faster dynamics in nanopores which is attributed to the reduced packing density as corroborated by the PALS measurements. This study shows that the dimensionality of the geometrical constraints plays a key role in the dynamics of confined systems.

ACKNOWLEDGMENTS

Financial support by SFB/TRR 102 within the project Polymers under multiple constraints: restricted and controlled molecular order and mobility is gratefully acknowledged.

[1] M. D. Ediger and J. A. Forrest, Macromolecules **47**, 471 (2014).
[2] F. Kremer, M. Tress, and E. U. Mapesa, J. Non-Cryst. Solids **407**, 277 (2015).
[3] F. Kremer, *Dynamics in Geometrical Confinement*, Advances in Dielectrics (Springer, London, 2014).
[4] A. Schönhals, H. Goering, C. Schick, B. Frick, and R. Zorn, Colloid Polym. Sci. **282**, 882 (2004).
[5] F. Kremer and A. Schönhals, *Broadband Dielectric Spectroscopy* (Springer, Berlin, 2003).
[6] S. Mirzaeifard and S. M. Abel, Soft Matter **12**, 1783 (2016).
[7] A. Serghei and F. Kremer, Rev. Sci. Instrum. **79**, 026101 (2008).
[8] M. Tress, E. U. Mapesa, W. Kossack, W. K. Kipnusu, M. Reiche, and F. Kremer, Science **341**, 1371 (2013).
[9] M. Elsayed, N. Y. Arutyunov, R. Krause-Rehberg, V. Emtsev, G. Oganesyan, and V. Kozlovski, Acta Mater. **83**, 473 (2015).
[10] J. Kansy, Nucl. Instrum. Methods Phys. Res., Sect. A **374**, 235 (1996).
[11] A. Schönhals, H. Goering, C. Schick, B. Frick, and R. Zorn, J. Non-Cryst. Solids **351**, 2668 (2005).
[12] A. Schönhals, H. Goering, C. Schick, B. Frick, M. Mayorova, and R. Zorn, Eur. Phys. J.: Spec. Top. **141**, 255 (2007).
[13] G. Carini, V. Crupi, G. D´Angelo, D. Majolino, P. Migliardo, and Y. Mel´nichenko, J. Chem. Phys. **107**, 2292 (1997).
[14] A. Patkowski, T. Ruths, and E. W. Fischer, Phys. Rev. E **67**, 021501 (2003).
[15] V. Crupi, D. Majolino, P. Migliardo, and V. Venuti, J. Phys. Chem. B **106**, 10884 (2002).
[16] B. Frick, C. Alba-Simionesco, G. Dosseh, C. L. Quellec, A. Moreno, J. Colmenero, A. Schönhals, R. Zorn, K. Chrissopoulou, S. Anastasiadis, and K. Dalnoki-Veress, J. Non-Cryst. Solids **351**, 2657 (2005).
[17] B. J. Loughnane, R. A. Farrer, A. Scodinu, T. Reilly, and J. T. Fourkas, J. Phys. Chem. B **104**, 5421 (2000).
[18] R. A. Farrer and J. T. Fourkas, Acc. Chem. Res. **36**, 605 (2003).
[19] A. Schönhals, H. Goering, K. W. Brzezinka, and C. Schick, J. Phys.: Condens. Matter **15**, S1139 (2003).
[20] M. Arndt, R. Stannarius, W. Gorbatschow, and F. Kremer, Phys. Rev. E **54**, 5377 (1996).

[21]R. Richert and M. Yang, J. Phys. Chem. B **107**, 895 (2003).
[22]A. R. Brás, E. G. Merino, P. D. Neves, I. M. Fonseca, M. Dionísio, A. Schönhals, and N. T. Correia, J. Phys. Chem. C **115**, 4616 (2011).
[23]W. K. Kipnusu, W. Kossack, C. Iacob, M. Jasiurkowska, J. Sangoro, and F. Kremer, Z. Phys. Chem. **226**, 797 (2012).
[24]M. Eldrup, D. Lightbody, and J. Sherwood, Chem. Phys. **63**, 51 (1981).
[25]W. K. Kipnusu, M. Elsayed, W. Kossack, S. Pawlus, K. Adrjanowicz, M. Tress, E. U. Mapesa, R. Krause-Rehberg, K. Kaminski, and F. Kremer, J. Phys. Chem. Lett. **6**, 3708 (2015).
[26]K. Adrjanowicz, K. Kaminski, K. Koperwas, and M. Paluch, Phys. Rev. Lett. **115**, 265702 (2015).
[27]M. Tarnacka, W. K. Kipnusu, E. Kaminska, S. Pawlus, K. Kaminski, and M. Paluch, Phys. Chem. Chem. Phys. **18**, 23709 (2016).